Supplemental material to this article can be found at:
http://molpharm.aspetjournals.org/content/suppl/2005/03/08/mol.104.006734.DC1.html

0026-895X/05/6703-798–805$20.00
MOLECULAR PHARMACOLOGY
Copyright © 2005 The American Society for Pharmacology and Experimental Therapeutics
Mol Pharmacol 67:798–805, 2005

Vol. 67, No. 3
22/1193669
Printed in U.S.A.

Activation of the Melastatin-Related Cation Channel TRPM3 by D-*erythro*-Sphingosine

Christian Grimm, Robert Kraft, Günter Schultz, and Christian Harteneck

Institut für Pharmakologie, Charité Campus Benjamin Franklin, Berlin, Germany

Received August 30, 2004; accepted November 18, 2004

ABSTRACT

TRPM3, a member of the melastatin-like transient receptor potential channel subfamily (TRPM), is predominantly expressed in human kidney and brain. TRPM3 mediates spontaneous Ca^{2+} entry and nonselective cation currents in transiently transfected human embryonic kidney 293 cells. Using measurements with the Ca^{2+}-sensitive fluorescent dye fura-2 and the whole-cell patch-clamp technique, we found that D-*erythro*-sphingosine, a metabolite arising during the de novo synthesis of cellular sphingolipids, activated TRPM3. Other transient receptor potential (TRP) channels tested [classic or canonical TRP (TRPC3, TRPC4, TRPC5), vanilloid-like TRP (TRPV4, TRPV5, TRPV6), and melastatin-like TRP (TRPM2)] did not significantly respond to application of sphingosine. Sphingosine-induced TRPM3 activation was not mediated by inhibition of protein kinase C, depletion of intracellular Ca^{2+} stores, and intracellular conversion of sphingosine to sphingosine-1-phosphate. Although sphingosine-1-phosphate and ceramides had no effect, two structural analogs of sphingosine, dihydro-D-*erythro*-sphingosine and *N*,*N*-dimethyl-D-*erythro*-sphingosine, also activated TRPM3. Sphingolipids, including sphingosine, are known to have inhibitory effects on a variety of ion channels. Thus, TRPM3 is the first ion channel activated by sphingolipids.

Transient receptor potential (TRP) proteins form a superfamily of nonselective cation channels containing six putative transmembrane domains, with the pore-forming region between the fifth and sixth segment, and cytosolic C and N termini (Clapham, 2003). Three main subfamilies of TRP channels have been described: TRPC (C for "classic" or "canonical"), TRPV (V for vanilloid receptor-like), and TRPM (M for melastatin-like) (Montell et al., 2002b). TRP members are expressed in a variety of organisms and cell types and are activated by various signals from both inside and outside the cell, such as hormones, temperature, cell swelling, Ca^{2+}, and endogenous or synthetic ligands (Montell et al., 2002a; Clapham, 2003). Thereby, ligand-mediated regulation is the most frequently observed activation mechanism within the TRP superfamily. Arachidonic acid (AA) and linolenic acid were shown to activate *Drosophila melanogaster* TRP and TRPL channels (Chyb et al., 1999). Other lipid mediators, such as diacylglycerol analogs, were described to open the mammalian TRPC channels TRPC3, TRPC6, and TRPC7 (Hofmann et al., 1999; Okada et al., 1999). TRPV1 and the related channel TRPV4 have been shown to be opened by the endocannabinoid anandamide and its metabolite arachidonic acid (Zygmunt et al., 1999; Watanabe et al., 2003). Products of the lipoxygenase and cytochrome P450 epoxygenase pathways of the arachidonic acid metabolism were identified as potent activators of TRPV1 and TRPV4, respectively (Hwang et al., 2000; Watanabe et al., 2003).

We have recently characterized a TRPM3 variant containing 1325 aa as a spontaneously active, Ca^{2+}-permeable cation channel, which is stimulated by hypotonic cell swelling (Grimm et al., 2003). This TRPM3 variant was cloned from human fetal brain, and its native expression in human brain and kidney was confirmed by Western blot analysis using a specific TRPM3 antibody (Grimm et al., 2003). The swelling-

The study was supported by the Deutsche Forschungsgemeinschaft, Fonds der Chemischen Industrie, and Sonnenfeld-Stiftung.
C.G. and R.K. contributed equally to this study.
Article, publication date, and citation information can be found at http://molpharm.aspetjournals.org.
doi:10.1124/mol.104.006734.

ABBREVIATIONS: TRP, transient receptor potential; TRPC, classic or canonical transient receptor potential; TRPV, vanilloid receptor-like transient receptor potential; TRPM, melastatin-like transient receptor potential; AA, arachidonic acid; aa, amino acid; PLC, phospholipase C; BAPTA, 1,2-bis(2-aminophenoxy)ethane-*N*,*N*,*N*′,*N*′-tetraacetic acid; SPH, D-*erythro*-sphingosine; S1P, D-*erythro*-sphingosine-1-phosphate; $[Ca^{2+}]_i$, intracellular calcium concentration; HEK, human embryonic kidney; $NMDG^+$, *N*-methyl-D-glucamine; DHS, dihydro-D-*erythro*-sphingosine; DMS, *N*,*N*-dimethyl-D-*erythro*-sphingosine; C2-Cer, *N*-acetyl-D-*erythro*-sphingosine; C8-Cer, *N*-octanoyl-D-*erythro*-sphingosine; Gö 6976, 12-(2-cyanoethyl)-6,7,12,13-tetrahydro-13-methyl-5-oxo-5*H*-indolo(2,3-*a*)pyrrolo(3,4-*c*)-carbazole; BIM I, 2-[1-(3-dimethylaminopropyl)-1*H*-indol-3-yl]-3-(1*H*-indol-3-yl)-maleimide; AEA, anandamide; LNA, linolenic acid; LA, linoleic acid; OAG, 1-oleoyl-2-acetyl-sn-glycerol; NT, nontransfected; DDG, 1,2-didecanoyl-rac-glycerol; IP_3, inositol 1,4,5-trisphosphate; PKC, protein kinase C; I_{CRAC}, calcium release-activated calcium current; EST, expressed sequence tag; SPHK, sphingosine kinase.

MOLECULAR PHARMACOLOGY

Downloaded from molpharm.aspetjournals.org at ASPET Journals on May 20, 2015

induced activation of another TRP channel, TRPV4, has been shown to be based on the formation of AA and its derivative 5′,6′-epoxyeicosatrienoic acid (Vriens et al., 2003). Although fatty acids or lipid metabolites from the phospholipase C (PLC) and phospholipase A_2 pathway were ineffective as activators of TRPM3, we found an activation of TRPM3 by the sphingolipid D-*erythro*-sphingosine (SPH) and by SPH analogs. SPH is a central metabolite arising during the de novo synthesis of cellular sphingolipids. The equilibrium of ceramides, SPH, and D-*erythro*-sphingosine-1-phosphate (S1P) plays a key role in regulating growth, differentiation, survival, and cell death (Huwiler et al., 2000). Members of the melastatin subfamily of TRP channels are apparently involved in cell death and regulation of cell proliferation (Duncan et al., 1998; Hara et al., 2002; Aarts et al., 2003; Hanano et al., 2004). In contrast to SPH, neither ceramides nor S1P, AA, or diacylglycerol analogs were able to stimulate TRPM3. We show here for the first time that an ion channel, TRPM3, is activated by SPH and may be involved in SPH-induced Ca^{2+} entry in a multiplicity of cellular systems.

Materials and Methods

Cell Culture and Transfections. HEK293 cells were cultured in Earle's minimal essential medium (Biochrom, Berlin, Germany), supplemented with 10% fetal calf serum (Biochrom), 100 μg/ml penicillin, and 100 μg/ml streptomycin under 5% CO_2 atmosphere at 37°C. Cells were plated in 85-mm dishes onto glass coverslips and transiently transfected with 1.5 to 2 μg of DNA and 5 μl of FuGENE 6 transfection reagent (Roche Diagnostics, Indianapolis, IN) in 95 μl of Opti-MEM medium vector (Invitrogen, Groningen, The Netherlands) 48 h later. The cDNAs of the following TRP channels C-terminally fused to enhanced green or yellow fluorescent proteins were used: hsTRPC3 (GenBank accession number NM003305), mmTRPC4 (GenBank no. NM016984), mmTRPC5 (GenBank accession number NM009428), hsTRPV4 (GenBank accession number NM147204), mmTRPV5 (GenBank accession number XM112633), mmTRPV6 (GenBank accession number NM022413), hsTRPM2 (GenBank accession number NM003307), and hsTRPM3 (GenBank accession number AJ505026).

Fluorescence Measurements. Measurements of intracellular Ca^{2+} concentration ($[Ca^{2+}]_i$) in single cells were carried out using the fluorescent indicator fura-2 in combination with a monochromator-based imaging system (TILL Photonics, Gräfelfing, Germany) attached to an inverted microscope (Axiovert 100; Carl Zeiss, Oberkochen, Germany). HEK293 cells were loaded with 4 μM fura-2-AM (Molecular Probes, Leiden, The Netherlands) in a standard solution as described previously (Grimm et al., 2003). Osmolarity effects were studied in a solution with 88 instead of 138 mM NaCl, containing 0 and 100 mM mannitol, resulting in osmolarities of 200 and 300 mOsM, respectively. Fluorescence quenching by Mn^{2+} entry and $[Ca^{2+}]_i$ measurements were carried out as described previously (Grimm et al., 2003).

Patch-Clamp Measurements. Membrane currents were recorded in the whole-cell configuration of the patch-clamp technique, using an Axopatch 200B amplifier (Axon Instruments Inc., Union City, CA), subsequently low-pass filtered at 1 kHz, digitized with a sampling rate of 5 kHz, and analyzed using pCLAMP software (version 7.0; Axon Instruments Inc.). The pipette resistance varied between 3 and 5 MΩ. Pipettes were filled with a solution composed of 130 mM $CsCH_3O_3S$, 10 mM CsCl, 5 mM $MgCl_2$, 10 mM HEPES, and 10 mM BAPTA (pH adjusted to 7.2 with CsOH). The bath solution contained 140 mM NaCl, 2 mM $CaCl_2$, 1 mM $MgCl_2$, 10 mM glucose and 10 mM HEPES (pH adjusted to 7.4 with NaOH). For Na^+-free conditions, Na^+ was replaced with 140 mM *N*-methyl-D-glucamine ($NMDG^+$). In some experiments, extracellular solution contained 100 mM $CaCl_2$. Whole-cell currents were elicited by either voltage ramps (400-ms duration) applied every 5 s from a holding potential of 0 mV or by voltage steps as shown in Fig. 4. Voltage ramps were elicited from either −100 to +100 mV or +100 mV to −100 mV. Relative cation permeabilities were calculated as described previously (Grimm et al., 2003). All pooled data from patch-clamp experiments are expressed as means ± S.E.M. from *n* cells.

Chemicals. SPH, dihydro-D-*erythro*-sphingosine (DHS), *N*,*N*-dimethyl-D-*erythro*-sphingosine (DMS), *N*-acetyl-D-*erythro*-sphingosine (C2-Cer), and *N*-octanoyl-D-*erythro*-sphingosine (C8-Cer) (Calbiochem, San Diego, CA) were diluted from 20 mM stock solutions in ethanol, S1P (Calbiochem) from a 10 mM stock solution in methanol, AA, and anandamide (AEA) (Sigma-Aldrich, St. Louis, MO) from 50 mM stock solutions in ethanol, linolenic acid (LNA), and linoleic acid (LA) (Sigma-Aldrich) from 100 mM stock solutions in ethanol, 1-oleoyl-2-acetyl-*sn*-glycerol (OAG), and 1,2-didecanoyl-rac-glycerol (DDG) (Calbiochem) from 100 mM stock solutions in dimethyl sulfoxide.

Results

Activation of TRPM3 by SPH. Extracellular application of SPH (20 μM) induced an increase in $[Ca^{2+}]_i$ in TRPM3-transfected HEK293 cells within 20 to 30 s after start of application, whereas nontransfected control cells (NT) showed only very small responses (Fig. 1A). Exchange of extracellular Ca^{2+} for EGTA (2 mM) almost completely inhibited these $[Ca^{2+}]_i$ increases, indicating Ca^{2+} influx via the plasma membrane (Fig. 1A). In the presence of EGTA and before adding extracellular Ca^{2+}, SPH induced no effects in TRPM3-transfected HEK293 cells (Fig. 1B). In fura-2 quench experiments using 200 μM Mn^{2+}, the spontaneous activity of TRPM3-transfected HEK293 cells was enhanced after application of 20 μM SPH, whereas nontransfected control cells showed only weak effects (Fig. 1C). The concentration of SPH for half-maximal activation of TRPM3 was 12 μM obtained from increases in $[Ca^{2+}]_i$ (Fig. 1D). Application of SPH (20 μM) as well as application of hypotonic extracellular solution each produced increases in $[Ca^{2+}]_i$ with comparable amplitudes in individual cells (Fig. 1E). Peak values of SPH-induced increases in $[Ca^{2+}]_i$ in TRPM3-transfected cells were not exceeded by additional application of hypotonic extracellular solution (200 mOsM) (Fig. 1F). This suggests that treatment with 20 μM SPH and hypotonic stimulation is not additive.

Specificity of the TRPM3 Activation by SPH. In contrast to TRPM3, other members of the TRP family transiently transfected in HEK293 cells (hsTRPC3, mmTRPC4, mmTRPC5, hsTRPV4, mmTRPV5, mmTRPV6, and hsTRPM2) were not significantly activated by SPH compared with nontransfected control cells (Fig. 2A). Diverse TRP channels are activated by fatty acids or lipids, particularly by products of the phospholipase C and phospholipase A_2 pathway (Chyb et al., 1999, Hofmann et al., 1999; Okada et al., 1999). We therefore examined a possible activation of TRPM3 by such substances. However, no significant differences were detectable in TRPM3-transfected cells compared with nontransfected control cells upon application (100 μM each) of AEA, AA, LNA, LA, OAG, or DDG (Fig. 2B). A TRP channel distantly related to TRPM3, TRPC3, has been described to be activated by diacylglycerol analogs (Hofmann et al., 1999). In parallel fura-2 experiments, the effects of the diacylglycerol analog DDG and SPH were tested in HEK293 cells transiently transfected with either TRPC3 or TRPM3

Downloaded from molpharm.aspetjournals.org at ASPET Journals on May 20, 2015

(Fig. 2C). Although TRPC3-expressing cells clearly responded to application of 100 μM DDG, 20 μM SPH did not significantly increase $[Ca^{2+}]_i$ in these cells (Fig. 2D). On the other hand, in TRPM3-expressing cells the $[Ca^{2+}]_i$ was not significantly elevated by application of 100 μM DDG. Instead, 20 μM SPH increased $[Ca^{2+}]_i$ in TRPM3-expressing cells (Fig. 2E).

SPH Induced Currents through TRPM3. In TRPM3-transfected cells, extracellular SPH (10 μM) induced whole-cell currents that could be resolved on the single-channel level during the onset of activation within a time period of about 30 s after start of application (Fig. 3A). At a holding potential of -60 mV, single channel openings with an amplitude of about -4.5 pA ($n = 3$) were detected, corresponding to a chord conductance of 75 pS. From the current-voltage relationship of the SPH-induced single channel currents, we calculated a slope conductance of 73 pS for inward currents (Fig. 3B). Current-voltage relationships of SPH-induced whole-cell currents during voltage-ramps (starting from negative potentials) showed a clear outward rectification (Fig. 3C). Exchange of extracellular Na^+-containing solution for 100 mM $CaCl_2$ induced a rapid and transient increase in SPH-induced inward currents and a shift of the reversal potential toward more positive voltages (Fig. 3C). Application of a solution containing $NMDG^+$ suppressed these inward currents, indicating permeation of Ca^{2+} through TRPM3 channels (Fig. 3C). Figure 3D shows the voltage dependence of the current densities under different ionic conditions. In the presence of Na^+-containing bath solution, the mean currents were -9.3 ± 2.4 and 33.3 ± 5.8 pA/pF ($n = 10$) at -100 mV and $+100$ mV, respectively. In the presence of 100 mM $CaCl_2$, current densities were -59.3 ± 7.2 and 47.2 ± 5.6 pA/pF ($n = 10$), respectively. To explore a possible voltage modulation of TRPM3, we applied 500-ms voltage steps from a holding potential of 0 mV. During application of SPH on TRPM3-transfected cells, currents showed a time-dependent increase during prolonged depolarization and a decrease during hyperpolarization (Fig. 4A). Current-voltage relationships observed during different test potentials after a prestep to $+100$ mV revealed a linear voltage dependence of instantaneous currents (Fig. 4B), similarly to the instantaneous currents through the voltage-dependent channels TRPM4 and TRPM8 (Nilius et al., 2003; Voets et al., 2004). However, in contrast to currents through TRPM4 and TRPM8, we did not find a complete deactivation of TRPM3-mediated inward currents at negative test potentials and holding potentials of 0 mV (Fig. 4B) or -90 mV (data not shown). To investigate a possible voltage dependence of TRPM3 open probability, we measured the current amplitude during a voltage step to -100 mV after different presteps (Fig. 4C). The fraction of open channels (F_{open}) at the end of each prestep potential was calculated by normalizing the current amplitudes at the beginning of the step to -100 mV to their maximal value. The resulting F_{open}-voltage relationships could be fitted by a Boltzmann function (Fig. 4C), as described previously (Nilius et al., 2003). The mean slope of these fits, obtained from individual TRPM3-transfected cells treated with 10 μM SPH, was 22.3 ± 1.7 mV ($n = 6$). The voltage for half-maximal activation varied from cell to cell and ranged from -67 to $+113$ mV. To investigate the relative cation permeability of SPH-activated TRPM3 channels, we applied voltage ramps from $+100$ to -100 mV after 500-ms-long prepulses to $+100$

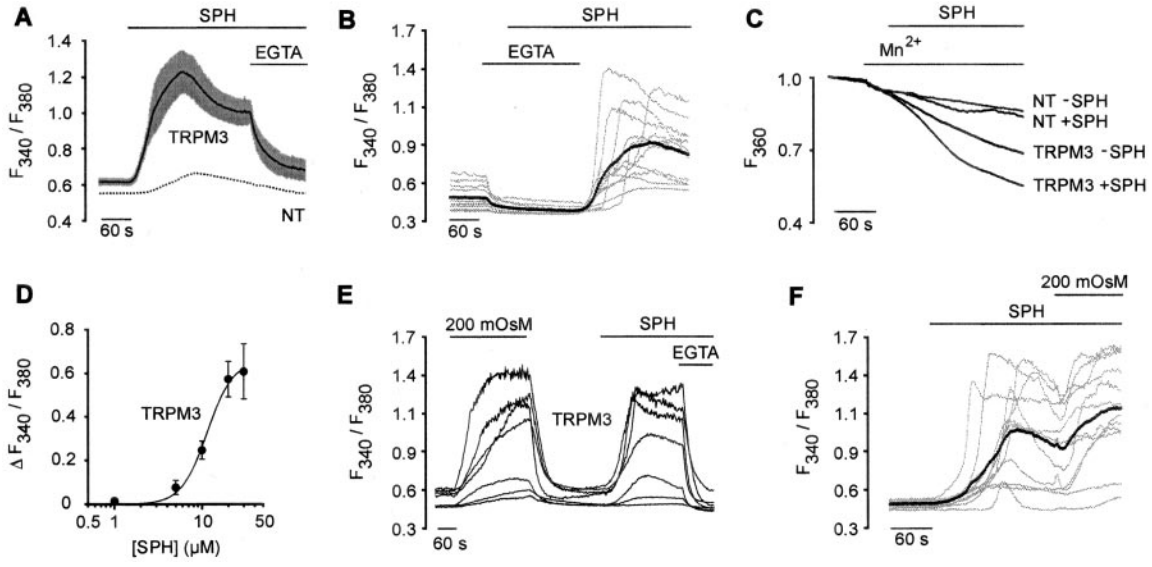

Fig. 1. TRPM3 is activated by SPH in HEK293 cells. A, effect of 20 μM SPH on $[Ca^{2+}]_i$ in TRPM3-transfected cells. The black line indicates mean values from eight independent experiments with at least 20 cells each. Gray areas depict the S.E.M. for each data point. The dotted line represents mean values from eight independent experiments with at least 20 NT cells each. During application of SPH, 2 mM extracellular Ca^{2+} was exchanged for 2 mM EGTA. B, effect of 20 μM SPH on $[Ca^{2+}]_i$ in TRPM3-transfected cells in the presence of 2 mM EGTA and after addition of 2 mM extracellular Ca^{2+}. Shown are single cell traces from one representative fura-2 experiment of three independent experiments with at least 20 cells each (mean value in black). C, Mn^{2+} influx in TRPM3-transfected cells was enhanced by application of 20 μM SPH. Shown are mean values of three independent experiments with at least 15 cells each. The concentration of Mn^{2+} was 200 μM. D, concentration-response curve for the increase in $[Ca^{2+}]_i$ by SPH. Data points (mean $\pm$ S.E.M. of n independent experiments with at least 20 cells each) were calculated from the SPH-induced responses 200 s after application of 1 μM ($n = 4$), 5 μM ($n = 4$), 10 μM ($n = 13$), 20 μM ($n = 14$), and 30 μM ($n = 6$). The concentration of SPH giving a half-maximal increase in $[Ca^{2+}]_i$ was 12 μM. E, stimulation of single TRPM3-transfected cells with hypotonic extracellular solution (200 mOsM) or with 20 μM SPH (in 300 mOsM) each increased $[Ca^{2+}]_i$. During application of SPH, 2 mM extracellular Ca^{2+} was exchanged for 2 mM EGTA. F, subsequent application of 20 μM SPH and hypotonic extracellular solution (200 mOsM). Shown are traces of TRPM3-transfected cells from one representative fura-2 experiment of three independent experiments with at least 20 cells each (mean value in black).

Downloaded from molpharm.aspetjournals.org at ASPET Journals on May 20, 2015

mV. Under these conditions, a hyperpolarization-induced deactivation of TRPM3 should be attenuated. Indeed, upon application of SPH the current activation was much steeper (Fig. 4D) than in continuous recordings at −60 mV (Fig. 3A) or in conventional voltage ramp recordings (Fig. 3C). Exchange of Na^+-containing solution for 100 mM $CaCl_2$ shifted the reversal potentials of the current-voltage relationships from +1.2 ± 2.0 mV (n = 5) to +10.2 ± 4.4 mV (n = 5) (Fig. 4D). Application of 140 mM NMDG-Cl nearly completely abolished inward currents, suggesting permeation through a cation channel. From the shifts of the reversal potentials during subsequent application of Na^+ and Ca^{2+}, a relative permeability P_{Ca}/P_{Na} = 1.91 ± 0.51 (n = 5) was calculated. The ion concentrations were corrected for the respective activity coefficients (0.76 for 140 mM NaCl, 0.517 for 100 mM $CaCl_2$).

Effects of SPH after Store Depletion, Inhibition of Inositol 1,4,5-Trisphosphate (IP_3) Receptors or Inhibition of Protein Kinase C (PKC). To test whether TRPM3 activation by SPH is independent of Ca^{2+} store depletion, we

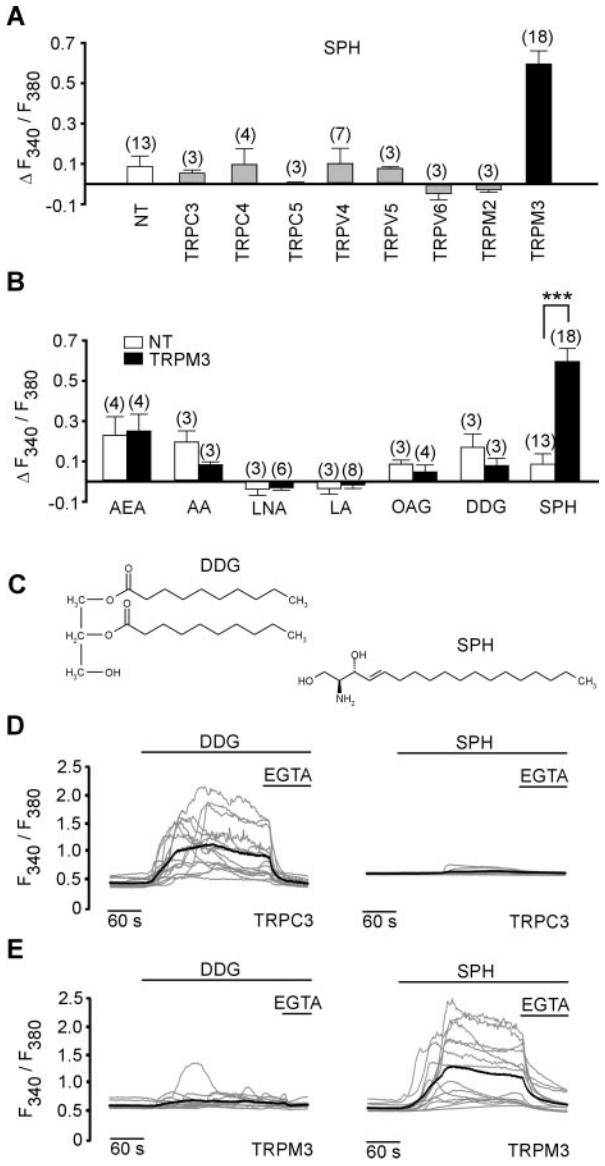

Fig. 2. Sphingosine is a specific stimulus for TRPM3. A, effects of 20 μM SPH on HEK293 cells transfected with diverse TRP channels C-terminally fused to enhanced green or yellow fluorescent protein: hsTRPC3, mmTRPC4, mmTRPC5, hsTRPV4, mmTRPV5, mmTRPV6, hsTRPM2, and hsTRPM3. Columns represent the SPH-induced increases in $[Ca^{2+}]_i$ 200 s after application of SPH as means ± S.E.M. of at least three independent fura-2 experiments with at least 20 cells each. B, effects of different fatty acids and lipids (AEA, AA, LNA, LA, OAG, and DDG; 100 μM each) on TRPM3-transfected cells (filled columns) and nontransfected cells (open columns). Data were calculated from lipid-mediated increases in $[Ca^{2+}]_i$ 200 s after start of application, shown as means ± S.E.M. of at least three independent fura-2 experiments each. ***, $p < 0.001$, compared with nontransfected cells. C, chemical structures of the lipids DDG and SPH. D, effects of either DDG (100 μM) or SPH (20 μM) on HEK293 cells transfected with hsTRPC3. Shown are traces from representative fura-2 experiments with at least 15 cells each (mean value in black). E, effects of either DDG (100 μM) or SPH (20 μM) on HEK293 cells transfected with TRPM3. Shown are traces from representative experiments with at least 15 cells each (mean value in black).

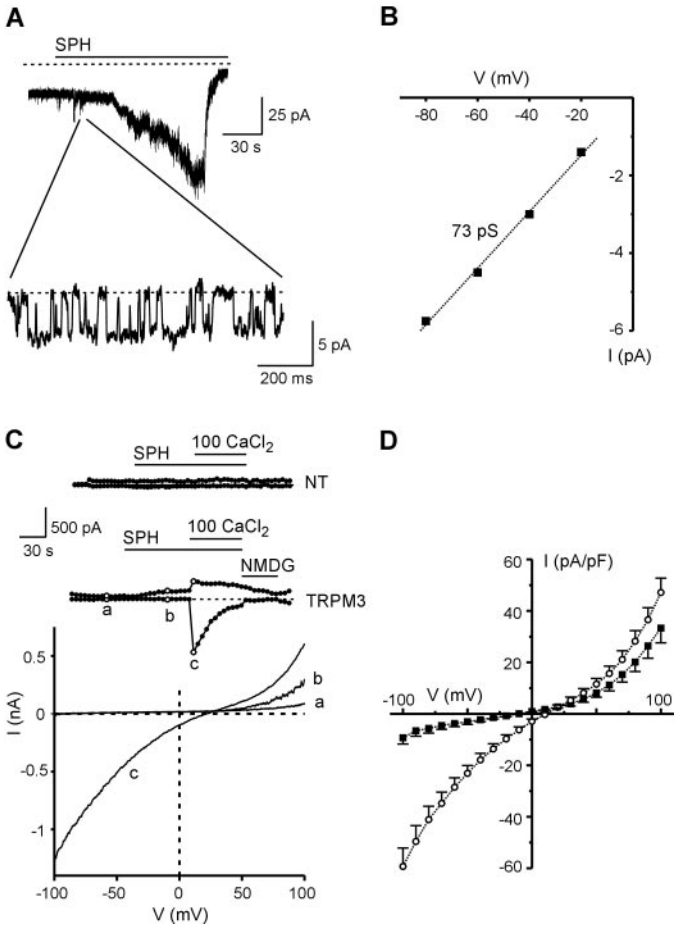

Fig. 3. Activation of TRPM3-mediated currents by SPH and by extracellular Ca^{2+}. A, whole-cell currents were continuously recorded from a TRPM3-transfected cell at a holding potential of −60 mV. After application of 10 μM SPH, single channel openings were resolved during a 1-s time interval. B, current-voltage relationship of SPH-induced single channel currents obtained from whole-cell recordings as shown in A. Each point represents mean values of single channel currents from independent experiments on one to three cells. C, currents were recorded from a TRPM3-transfected and an NT cell during voltage ramps from −100 to +100 mV (400-ms duration) at a holding potential of 0 mV. The insets above show the time courses of currents at −80 and +80 mV obtained from the voltage ramps. Extracellular Na^+-containing solution was substituted by either 100 mM $CaCl_2$ or 140 mM NMDG-Cl. Current-voltage relationships were obtained from responses before (a) and during (b) application of SPH and in the presence of 100 mM $CaCl_2$ and SPH (c). D, current-voltage relationships of SPH-induced currents obtained from recordings as shown in C were normalized to the cell capacitance. Data points represent mean current densities ± S.E.M. from 10 cells in the presence of Na^+-containing solution (solid squares) and 100 mM $CaCl_2$ (open circles).

Downloaded from molpharm.aspetjournals.org at ASPET Journals on May 20, 2015

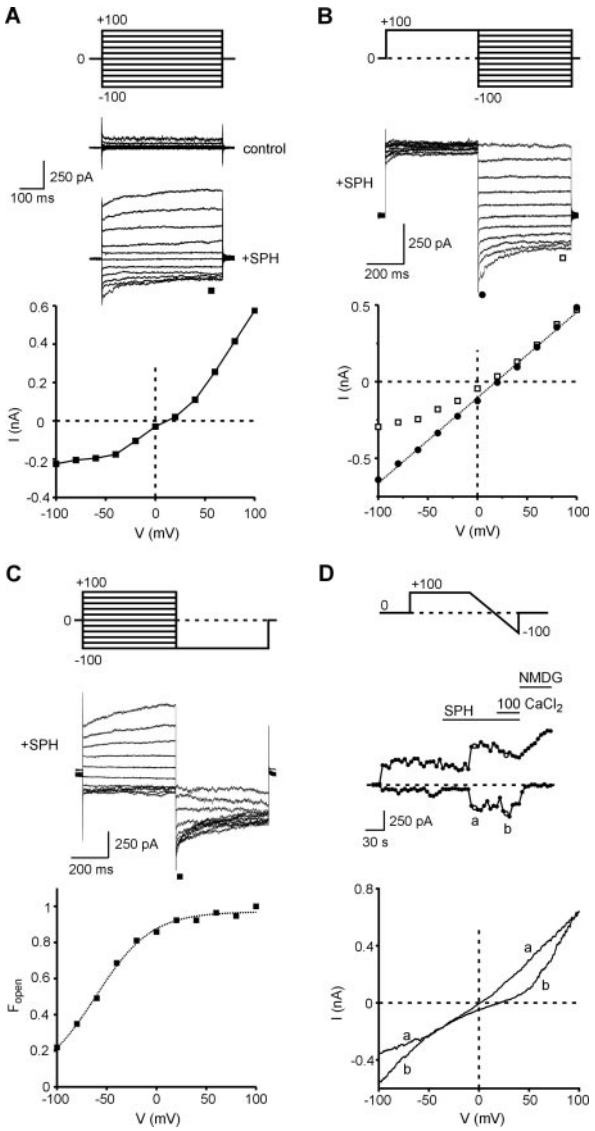

Fig. 4. Activation of TRPM3-mediated currents by depolarization. A, 500-ms voltage steps were applied from a holding potential of 0 mV to test potentials between −100 and +100 mV (increments of +20 mV). Corresponding whole-cell currents were recorded from a TRPM3-transfected cell during application of 10 μM SPH. The current-voltage relationship was constructed from the current amplitudes, obtained 450 ms after start of respective voltage-steps. B, a 500-ms prestep was followed by 500-ms voltage steps between −100 and +100 mV (increments of +20 mV). Currents were recorded from a TRPM3-transfected cell during application of 10 μM SPH. Current-voltage relationships were constructed from the current amplitudes, obtained 1 ms (solid circles) and 450 ms (open squares) after start of respective voltage steps. The dotted line represents a linear fit. C, 500-ms voltage presteps between −100 and +100 mV (increments of +20 mV) were followed by a 500-ms voltage step to −100 mV. Currents were recorded from a TRPM3-transfected cell during application of 10 μM SPH. The fraction of open channels (F_{open}) was calculated by normalizing the current amplitudes, obtained 1 ms after start of the step to −100 mV, to their maximal value. The dotted line represents a fit to a Boltzmann function of the form $F_{open} = F_{const} + (1 - F_{const})/(1 + \exp((V - V_{1/2})/s))$, where F_{open} represents the fraction of open channels at the prestep potential V, $V_{1/2}$ is the potential of half-maximal activation, s is the slope parameter, and F_{const} is the fraction of open channels at negative potentials. The fit yielded the following parameters: $F_{const} = 0.03$, s = 27.9 mV, $V_{1/2} = -61$ mV. D, currents were recorded from a TRPM3-transfected cell during voltage ramps from +100 mV to −100 mV (400-ms duration) after a 500-ms prepulse to +100 mV (see voltage protocol described above). The holding potential was 0 mV. The inset shows the time course of currents at −80 mV obtained from the voltage ramps. Extracellular Na^+-containing solution was substituted by either 100 mM $CaCl_2$ or 140 mM NMDG-Cl. Current-voltage relationships were obtained from responses at corresponding time points (a and b).

used thapsigargin (5 μM), an inhibitor of smooth endoplasmic reticulum Ca^{2+}-ATPase, which induces store-operated Ca^{2+} entry. SPH, described to inhibit calcium release-activated calcium current (I_{CRAC}) in RBL-2H3 cells (Mathes et al., 1998), blocked the thapsigargin-evoked Ca^{2+} signals in nontransfected HEK293 cells (Fig. 5A), whereas it induced $[Ca^{2+}]_i$ increases in TRPM3-transfected cells (Fig. 5B). To exclude a possible involvement of IP_3 receptors in SPH-mediated activation of TRPM3, we applied the IP_3 receptor inhibitor xestospongin C (1 μM). However, responses to SPH were not influenced by pretreatment with xestospongin C (Fig. 5C). SPH has originally been described as an inhibitor of PKC (Smith et al., 2000). Application of several known PKC inhibitors [i.e., 2-[1-(3-dimethylaminopropyl)-1*H*-indol-3-yl]-3-(1*H*-indol-3-yl)-maleimide (BIM I) (1 μM; Fig. 5D), calphostin C, or Gö 6976 (1 μM each; data not shown), and of an inhibitor of protein kinases, staurosporine (1 μM; Fig. 5D)] did not induce significant changes in $[Ca^{2+}]_i$ in TRPM3-transfected cells compared with nontransfected cells.

Effects of Other Sphingolipids. We tested sphingolipids from the sphingomyelin pathway that are structurally related to SPH (Fig. 6A). DHS and DMS also induced increases in $[Ca^{2+}]_i$ (Fig. 6B). No significant effects were measured after external application of the membrane-permeable ceramides C2-Cer (20 μM) and C8-Cer (20 μM) and of S1P (10 μM) (Fig. 6C). Extracellularly applied S1P produced a similar increase in $[Ca^{2+}]_i$ both in TRPM3-transfected and nontransfected cells, probably because of an activation of G protein-coupled S1P receptors that are endogenously expressed in HEK293 cells (Meyer zu Heringdorf et al., 2001). To test for a possible S1P-mediated activation of TRPM3 from the intracellular side, we perfused TRPM3-transfected cells with S1P (10 μM) via the patch pipette. During a time interval of

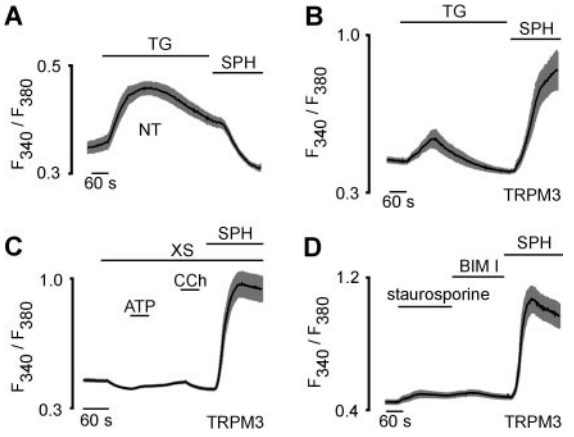

Fig. 5. Stimulation of TRPM3 by SPH is not mediated by store depletion, IP_3 receptor activation, or PKC inhibition. Effects of SPH application in NT cells (A) and in TRPM3-transfected HEK293 cells (B) after pretreatment with thapsigargin (TG; 5 μM). Responses are shown as mean (black line) ± S.E.M. (gray area) of one representative experiment from five similar experiments with at least 20 cells, each. C, SPH-induced responses in TRPM3-transfected cells after treatment with the IP_3 receptor inhibitor xestospongin C (XS; 1 μM). During treatment with xestospongin C, no ATP- and carbachol (CCh)-induced Ca^{2+} responses were observed (100 μM each). Data are mean (black line) ± S.E.M. (gray area) of one representative experiment of three similar experiments with at least 20 cells each. D, shown are the effects of the protein kinases inhibitor staurosporine (1 μM), the PKC inhibitor BIM I (1 μM), and SPH (20 μM) on TRPM3-transfected HEK293 cells as mean (black line) ± S.E.M. (gray area) of one representative experiment of three similar experiments with at least 20 cells each.

Downloaded from molpharm.aspetjournals.org at ASPET Journals on May 20, 2015

at least 2 min after attaining the whole-cell configuration, no steady increase in currents could be observed ($n = 4$; Fig. 6D). Subsequent application of SPH (10 μM) via the bath solution induced currents with similar properties to those shown in Fig. 4D. To further exclude an activation of TRPM3 through intracellular conversion of SPH to S1P, we used DMS, which is also known as an inhibitor of sphingosine kinases, that specifically phosphorylate SPH to S1P (Edsall et al., 1998; Huwiler et al., 2000). However, pretreatment with DMS (10 μM; data not shown) was not able to reduce SPH evoked increases in $[Ca^{2+}]_i$ in TRPM3-transfected HEK293 cells, indicating that SPHK activity and phosphorylation of SPH to S1P are not required for TRPM3 activation.

Discussion

The present study shows that a previously described TRPM3 variant containing 1325 aa (Grimm et al., 2003) is activated by SPH, independently of PKC inhibition, formation of S1P, or intracellular Ca^{2+} store depletion.

Electrophysiological investigation of this TRPM3 variant yielded a single channel conductance for SPH-induced currents of about 75 pS. This is in accordance with the previously reported value of 83 pS for spontaneously active TRPM3 channels in the presence of extracellular Na^+ (Grimm et al., 2003). From whole-cell currents in the presence of either extracellular Na^+ or Ca^{2+}, a relative permeability $P_{Ca}/P_{Na} = 1.91$ was calculated. This value is close to the relative permeability $P_{Ca}/P_{Na} = 1.57$ determined for spontaneously active TRPM3 channels (Grimm et al., 2003). In the presence of 100 mM extracellular Ca^{2+}, the outward rectification of SPH-induced currents seems to be replaced by an inward and outward rectification, resulting in a S-like current-voltage relationship (Fig. 3D). SPH-induced currents elicited by voltage steps were characterized by an activation at positive potentials and a deactivation at negative potentials. This resembles the kinetic behavior of some other TRPM channels [i.e., TRPM4, TRPM5, and TRPM8 (Hofmann et al., 2003; Nilius et al., 2003; Voets et al., 2004)]. From fits to the Boltzman function, giving a value of about 22 mV for an e-fold increase in open probability, we suggest a voltage dependence of TRPM3 channels. The voltage for half-maximal activation of TRPM3 channels in the presence of 10 μM SPH, however, was very different between individual cells, ranging from -67 to $+113$ mV. Therefore, the definition of a SPH-induced shift of the activation curve at appropriate membrane potentials, as shown for the menthol- and temperature-dependent activation of TRPM8 (Voets et al., 2004), was not possible. The variable voltages for half-maximal activation of TRPM3 may be caused by differences in the distribution and binding of the lipid compound SPH to the channels in individual cells. Furthermore, the concentration of endogenous SPH inducing spontaneous activity of TRPM3 may vary from cell to cell.

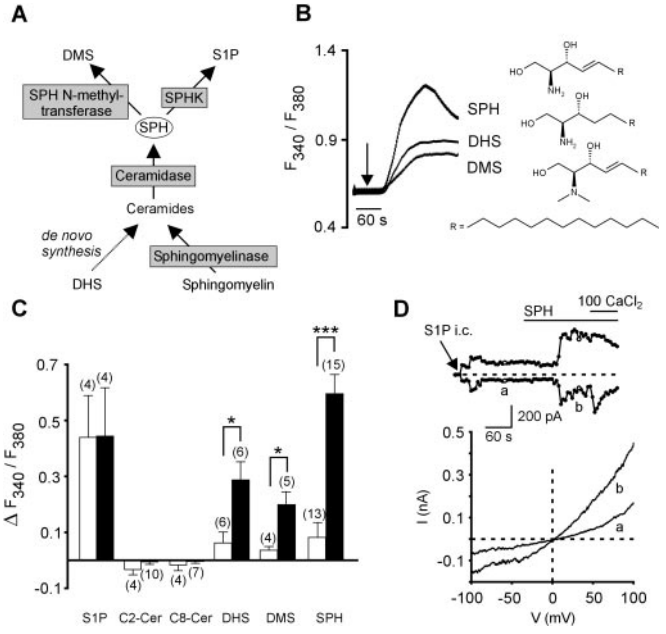

Fig. 6. Activation of TRPM3 by different sphingolipids. A, biosynthesis and degradation of sphingolipids (metabolizing enzymes shown in gray boxes; SPHK, sphingosine-kinase). B, effects of SPH ($n = 8$), DHS ($n = 6$), and DMS ($n = 5$) (20 μM each) on $[Ca^{2+}]_i$ in fura-2-loaded, TRPM3-transfected HEK293 cells. Traces represent means of n independent experiments with at least 20 cells, each. C, effects of diverse sphingolipids, including the membrane-permeable ceramides (C2- and C8-ceramide) on $[Ca^{2+}]_i$ in fura-2-loaded, TRPM3-transfected (filled columns) and nontransfected (open columns) cells. Data were calculated from sphingolipid-mediated responses 200 s after start of application, shown as means ± S.E.M. of n independent experiments. *, $p < 0.05$ and ***, $p < 0.001$, compared with nontransfected cells. D, whole-cell currents were recorded during voltage ramps from +100 to −100 mV (400-ms duration) after a 500-ms prepulse to +100 mV. The inset shows the time course of currents at −80 mV yielded from the voltage ramps. After obtaining the whole-cell configuration (arrow), the cell was perfused with a pipette solution containing 10 μM S1P. During application of 10 μM extracellular SPH, extracellular Na^+-containing solution was substituted by 100 mM $CaCl_2$. Current-voltage relationships were obtained from responses at corresponding time points (a and b).

Hofmann et al. (1999) reported that the intracellular release of diacylglycerols after activation of G protein-coupled receptors and PLC induces opening of TRPC3 and TRPC6 channels. In this approach, the rate of Mn^{2+} entry after extracellular application of DAG analogs was slower than after receptor stimulation (Hofmann et al., 1999). This slower activation kinetics could be explained by a delay caused by incorporation and accumulation of DAG analogs in the plasma membrane and/or the cytosol. In analogy, the long latency for activation of TRPM3 could also be caused by an action of SPH in a membrane-delimited manner or from the intracellular face of the channel. This was substantiated by Ca^{2+} imaging experiments, in which activation of TRPC3 by the DAG analog DDG showed the same kinetics as those for TRPM3 by SPH (Fig. 2, D and E).

Lee et al. (2003) have recently described six TRPM3 splice variants named TRPM3a to TRPM3f. Because of a shorter N terminus (153 aa) and a longer C terminus (382 aa) compared with our variant (Grimm et al., 2003), these proteins consist of 1545 to 1580 amino acids. TRPM3a to TRPM3f differ by small deletions and insertions (12–25 aa) in the N terminus or the pore-forming domain. One variant, TRPM3a, has been shown to mediate spontaneous Ca^{2+} entry after transfection in HEK293 cells (Lee et al., 2003). The different C-terminal ends of the TRPM3 variants described by Lee et al. (2003) and of our TRPM3 variant have been independently confirmed by mouse EST clones. EST accession AK173218 corresponds to the C-terminal ends of TRPM3a to TRPM3f (Lee et al., 2003), and EST accession AK051867 corresponds to the C terminus of our variant (Grimm et al., 2003). Whether this differential splicing may result in different activation mechanisms and physiological functions remains to be elucidated.

Downloaded from molpharm.aspetjournals.org at ASPET Journals on May 20, 2015

The involvement of TRP channels in the sphingolipid pathway has not been investigated to date, and TRPM3 is the first TRP superfamily member described to be activated by SPH and SPH analogs. We show here that a variety of other TRP channels of all three subfamilies are not significantly activated by SPH. Sphingolipids, in particular SPH, have been described to inhibit ion channels, such as voltage-gated Ca^{2+} channels (McDonough et al., 1994; Titievsky et al., 1998), the skeletal muscle ryanodine receptor (Needleman et al., 1997; Sharma et al., 2000), and channels mediating I_{CRAC} in RBL-2H3 cells (Mathes et al., 1998). The activation of an ion channel by SPH has not been shown so far.

Although structural analogs to SPH (e.g., DHS and DMS) activated TRPM3, ceramides and S1P had no effect. S1P is the ligand for a family of five G protein-coupled receptors ($S1P_1$–$S1P_5$). They are ubiquitously expressed, couple to various G proteins and regulate, for example, angiogenesis, vascular maturation, and cardiac development (Spiegel and Milstien, 2003). S1P generated from SPH through phosphorylation by SPHKs (Huwiler et al., 2000; Maceyka et al., 2002) plays a role as an intracellular second messenger with Ca^{2+} release activity (Ghosh et al., 1990; Young and Nahorski, 2002). In patch-clamp and calcium imaging experiments, we show that both intracellular and extracellular application of S1P does not activate TRPM3. We therefore conclude that activation of TRPM3 by SPH is independent of the phosphorylation of SPH to S1P.

The activation of the sphingomyelinase/ceramidase pathway, for example, by growth factors (Jacobs and Kester, 1993; Coroneos et al., 1995) or by cell swelling, may result in prolonged Ca^{2+} entry in cells endogenously expressing TRPM3. Activation of TRPV4 is reported to be based on swelling-induced activation of phospholipase A_2 and cytochrome P450 epoxygenase (Vriens et al., 2004). Cell swelling and hypotonic stress can also activate tyrosine kinases in cardiac myocytes (Sadoshima et al., 1996) and the receptor-tyrosine-kinase epidermal growth factor receptor in fibroblasts (Franco et al., 2004). Thus, cell swelling may induce activation of TRPM3 directly or indirectly by activation of the sphingomyelinase/ceramidase pathway, resulting in release and intracellular accumulation of SPH as breakdown product of sphingomyelin/ceramides whereby sphingomyelin accounts for approximately 10 to 15% of total cellular phospholipid content (Zager et al., 2000).

Finally, our data do not support any contribution of Ca^{2+} store depletion to the activation of TRPM3. The endogenous store-operated Ca^{2+} entry in nontransfected HEK293 cells was blocked by SPH, which is in agreement with the inhibitory action of SPH on I_{CRAC} in RBL-2H3 cells (Mathes et al., 1998). Depletion of intracellular Ca^{2+} stores induced by the activation of PLC through the release of IP_3 and the opening of endoplasmic IP_3 receptors has been confirmed in a large number of cell types. Formation of SPH (e.g., by activation of receptor tyrosine kinases) thus results in an inhibition of store-operated Ca^{2+} entry, whereas a compensatory Ca^{2+} influx may occur in TRPM3-expressing cells.

Acknowledgments

We thank Inge Reinsch for technical assistance, Tim Plant for critical reading of the manuscript, and Michael Schaefer for providing the TRPC4 and TRPC5 cDNAs.

References

Aarts M, Iihara K, Wie WL, Xiong ZG, Arundine M, Cerwinski W, MacDonald JF, and Tymianski M (2003) A key role for TRPM7 channels in anoxic neuronal death. *Cell* **115:**863–877.

Chyb S, Raghu P, and Hardie RC (1999) Polyunsaturated fatty acids activate the Drosophila light-sensitive channels TRP and TRPL. *Nature (Lond)* **397:**255–259.

Clapham DE (2003) TRP channels as cellular sensors. *Nature (Lond)* **426:**517–524.

Coroneos E, Martinez M, McKenna S, and Kester M (1995) Differential regulation of sphingomyelinase and ceramidase activities by growth factors and cytokines. Implications for cellular proliferation and differentiation. *J Biol Chem* **270:**23305–23309.

Duncan LM, Deeds J, Hunter J, Shao J, Holmgren LM, Woolf EA, Tepper RI, and Shyjan AW (1998) Down-regulation of the novel gene melastatin correlates with potential for melanoma metastasis. *Cancer Res* **58:**1515–1520.

Grimm C, Kraft R, Sauerbruch S, Schultz G, and Harteneck C (2003) Molecular and functional characterization of the melastatin-related cation channel TRPM3. *J Biol Chem* **278:**21493–21501.

Edsall LC, Van Brocklyn JR, Cuvillier O, Kleuser B, and Spiegel S (1998) *N,N*-Dimethylsphingosine is a potent competitive inhibitor of sphingosine kinase but not of protein kinase C: modulation of cellular levels of sphingosine 1-phosphate and ceramide. *Biochemistry* **37:**12892–12898.

Franco R, Lezama R, Ordaz B, and Pasantes-Morales H (2004) Epidermal growth factor receptor is activated by hyposmolarity and is an early signal modulating osmolyte efflux pathways in Swiss 3T3 fibroblasts. *Pflueg Arch Eur J Physiol* **447:**830–839.

Ghosh TK, Bian J, and Gill DL (1990) Intracellular calcium release mediated by sphingosine derivatives generated in cells. *Science (Wash DC)* **248:**1653–1656.

Hanano T, Hara Y, Shi J, Morita H, Umebayashi C, Mori E, Sumimoto H, Ito Y, Mori Y, and Inoue R (2004) Involvement of TRPM7 in cell growth as a spontaneously activated Ca^{2+} entry pathway in human retinoblastoma cells. *J Pharmacol Sci* **95:**403–419.

Hara Y, Wakamori M, Ishii M, Maeno E, Nishida M, Yoshida T, Yamada H, Shimizu S, Mori E, Kudoh J, et al. (2002) LTRPC2 Ca^{2+}-permeable channel activated by changes in redox status confers susceptibility to cell death. *Mol Cell* **9:**163–173.

Hofmann T, Chubanov V, Gudermann T, and Montell C (2003) TRPM5 is a voltage-modulated and Ca^{2+}-activated monovalent selective cation channel. *Curr Biol* **13:**1153–1158.

Hofmann T, Obukhov AG, Schaefer M, Harteneck C, Gudermann T, and Schultz G (1999) Direct activation of human TRPC6 and TRPC3 channels by diacylglycerol. *Nature (Lond)* **397:**259–263.

Huwiler A, Kolter T, Pfeilschifter J, and Sandhoff K (2000) Physiology and pathophysiology of sphingolipid metabolism and signaling. *Biochim Biophys Acta* **1485:** 63–99.

Hwang SW, Cho H, Kwak J, Lee SY, Kang CJ, Jung J, Cho S, Min KH, Suh YG, Kim D, et al. (2000) Direct activation of capsaicin receptors by products of lipoxygenases: endogenous capsaicin-like substances. *Proc Natl Acad Sci USA* **97:**6155–6160.

Jacobs LS and Kester M (1993) Sphingolipids as mediators of effects of platelet-derived growth factor in vascular smooth muscle cells. *Am J Physiol* **265:**C740–C747.

Lee N, Chen J, Sun L, Wu S, Gray KR, Rich A, Huang M, Lin JH, Feder JN, Janovitz EB, et al. (2003) Expression and characterization of human transient receptor potential melastatin 3 (hTRPM3). *J Biol Chem* **278:**20890–20897.

Maceyka M, Payne SG, Milstien S, and Spiegel S (2002) Sphingosine kinase, sphingosine-1-phosphate and apoptosis. *Biochim Biophys Acta* **1585:**193–201.

Mathes C, Fleig A, and Penner R (1998) Calcium release-activated calcium current (I_{CRAC}) is a direct target for sphingosine. *J Biol Chem* **273:**25020–25030.

McDonough PM, Yasui K, Betto R, Salviati G, Glembotski CC, Palade PT, and Sabbadini RA (1994) Control of cardiac Ca^{2+} levels. Inhibitory actions of sphingosine on Ca^{2+} transients and L-type Ca^{2+} channel conductance. *Circ Res* **75:**981–989.

Meyer zu Heringdorf D, Lass H, Kuchar I, Lipinski M, Alemany R, Rumenapp U, and Jakobs KH (2001) Stimulation of intracellular sphingosine-1-phosphate production by G-protein-coupled sphingosine-1-phosphate receptors. *Eur J Pharmacol* **414:**145–154.

Montell C, Birnbaumer L, and Flockerzi V (2002a) The TRP channels, a remarkably functional family. *Cell* **108:**595–598.

Montell C, Birnbaumer L, Flockerzi V, Bindels RJ, Bruford EA, Caterina MJ, Clapham DE, Harteneck C, Heller S, Julius D, et al. (2002b) A unified nomenclature for the superfamily of TRP cation channels. *Mol Cell* **9:**229–231.

Needleman DH, Aghdasi B, Seryshev AB, Schroepfer GJ Jr, and Hamilton SL (1997) Modulation of skeletal muscle Ca^{2+}-release channel activity by sphingosine. *Am J Physiol* **272:**C1465–C1474.

Nilius B, Prenen J, Droogmans G, Voets T, Vennekens R, Freichel M, Wissenbach U, and Flockerzi V (2003) Voltage dependence of the Ca^{2+}-activated cation channel TRPM4. *J Biol Chem* **278:**30813–30820.

Okada T, Inoue R, Yamazaki K, Maeda A, Kurosaki T, Yamakuni T, Tanaka I, Shimizu S, Ikenaka K, Imoto K, et al. (1999) Molecular and functional characterization of a novel mouse transient receptor potential protein homologue TRP7 Ca^{2+}-permeable cation channel that is constitutively activated and enhanced by stimulation of G protein-coupled receptor. *J Biol Chem* **274:**27359–27370.

Sadoshima J, Qiu Z, Morgan JP, and Izumo S (1996) Tyrosine kinase activation is an immediate and essential step in hypotonic cell swelling-induced ERK activation and c-fos gene expression in cardiac myocytes. *EMBO (Eur Mol Biol Organ) J* **15:**5535–5546.

Sharma C, Smith T, Li S, Schroepfer GJ Jr, and Needleman DH (2000) Inhibition of Ca^{2+} release channel (ryanodine receptor) activity by sphingolipid bases: mechanism of action. *Chem Phys Lipids* **104:**1–11.

Smith ER, Merrill AH, Obeid LM, and Hannun YA (2000) Effects of sphingosine and other sphingolipids on protein kinase C. *Methods Enzymol* **312:**361–373.

Downloaded from molpharm.aspetjournals.org at ASPET Journals on May 20, 2015

Spiegel S and Milstien S (2003) Sphingosine-1-phosphate: an enigmatic signalling lipid. *Nat Rev Mol Cell Biol* **4:**397–407.
Titievsky A, Titievskaya I, Pasternack M, Kaila K, and Tornquist K (1998) Sphingosine inhibits voltage-operated calcium channels in GH4C1 cells. *J Biol Chem* **273:**242–247.
Voets T, Droogmans G, Wissenbach U, Janssens A, Flockerzi V, and Nilius B (2004) The principle of temperature-dependent gating in cold- and heat-sensitive TRP channels. *Nature (Lond)* **430:**748–754.
Vriens J, Watanabe H, Janssens A, Droogmans G, Voets T, and Nilius B (2003) Cell swelling, heat and chemical agonists use distinct pathways for the activation of the cation channel TRPV4. *Proc Natl Acad Sci USA* **101:**396–401.
Watanabe H, Vriens J, Prenen J, Droogmans G, Voets T, and Nilius B (2003) Anandamide and arachidonic acid use epoxyeicosatrienoic acids to activate TRPV4 channels. *Nature (Lond)* **424:**434–438.
Young KW and Nahorski SR (2002) Sphingosine 1-phosphate: a Ca^{2+} release mediator in the balance. *Cell Calcium* **32:**335–341.
Zager RA, Burkhart KM, and Johnson A (2000) Sphingomyelinase and membrane sphingomyelin content: determinants of proximal tubule cell susceptibility to injury. *J Am Soc Nephrol* **11:**894–902.
Zygmunt PM, Petersson J, Andersson DA, Chuang H, Sorgard M, Di Marzo V, Julius D, and Hogestatt ED (1999) Vanilloid receptors on sensory nerves mediate the vasodilator action of anandamide. *Nature (Lond)* **400:**452–457.

Address correspondence to: Dr. Christian Harteneck, Institut für Pharmakologie, Charité Campus Benjamin Franklin, Thielallee 69-73, 14195 Berlin, Germany. E-mail: christian.harteneck@charite.de

Downloaded from molpharm.aspetjournals.org at ASPET Journals on May 20, 2015